The importance of a variable fibre packing density in modelling the tensile behaviour of single filament yarns

Aurelien Sibellas, Morgan Rusinowicz, Jerome Adrien, Damien Durville, Éric Maire

The Importance of a Variable Fibre Packing Density in Modelling the Tensile Behaviour of Single Filament Yarns

Aurélien Sibellas[a,b,*], Morgan Rusinowicz[a], Jérôme Adrien[a], Damien Durville[b], Eric Maire[a]

[a] *Université de Lyon, INSA Lyon, MATEIS CNRS UMR5510, F-69621 Villeurbanne, France*
[b] *MSSMat Laboratory, CentraleSupélec, CNRS UMR8579, Université Paris-Saclay, F-91190 Gif-sur-Yvette, France*

Abstract

A model able to reproduce the tensile response of single continuous-filament yarns based on parameters derived from geometrical descriptors is presented in this paper. Samples of yarns made of polyester and aramid fibres were scanned at rest using X-ray microtomography, allowing a detailed identification of their fibre orientation distributions for different twists. The variation of the fibre packing density along with yarn extension was characterized by means of additional scans carried out during tensile tests. An analytical model of the tensile response of these yarns, based on the orientation distribution function and the evolution of the packing density identified from microtomography is proposed and validated against experimental results, with good agreements.

Keywords: A. Yarn, B. Directional orientation, B. Mechanical Properties, C. Analytical modelling, X-ray microcomputed tomography

1. Introduction

Continuous polymer fibres can be twisted together to make filament yarns providing a good flexural and torsional flexibility for a high strength in the longitudinal direction. Such yarns are widely used every day in the industry and in domestic life, in the form of ropes, cables, fabrics and reinforcement in composite materials. The initial non-linear mechanical behaviour of these fibre assemblies is highly dependent on their arrangement. Mechanics of twisted continuous-filament yarns made of textile fibres have been studied extensively in the last century [1, 2, 3, 4, 5] but most of the classic models remain not easily applicable in an industrial context. Nevertheless, some authors have succeeded in constructing an energy-based theory [2] simplifying calculations of the yarn mechanical properties. The corresponding model was finally expressed in the framework of the Principle of Virtual Work by Leech [6]. Improvements of these theories over the years allowed complex geometries of fibre paths to be taken into account in the form of orientation density functions [7, 5, 8, 9]. Hence, ideal and irregular structures can be represented by their

*Corresponding Author
Email addresses: aurelien.sibellas@insa-lyon.fr (Aurélien Sibellas), morgan.rusinowicz@insa-lyon.fr (Morgan Rusinowicz), jerome.adrien@insa-lyon.fr (Jérôme Adrien), damien.durville@centralesupelec.fr (Damien Durville), eric.maire@insa-lyon.fr (Eric Maire)

distribution of fibre orientations which are used as input data for a mechanical model. In a previous paper [10], fibre trajectories in twisted yarns were investigated with a new method using X-ray microtomography. Fibre paths were determined using image processing techniques which led to a complete numerical reconstruction of the yarn studied. The orientation distributions were calculated for single-ply and multi-ply yarns with different torsions and compared to models of orientation density function from the literature.

The aim of this paper is to show the impact of considering the experimental orientation density functions (ODF) on the tensile behaviour of single and multi-ply yarns as input data for an analytical model. The considered model is based on a hypothesis relating the deformation of oriented fibre segments to the yarn extension. Different relationships were proposed in the literature either giving a specific deformation to the segment as a function of its orientation angle [4, 5] or using an average deformation for all the segments [11, 12] to reflect a better cooperation between them. The first approach involves a contraction ratio λ which is often set to 0.5 for an approximately constant volume deformation of the whole yarn. However, studies showed that the radius of yarns under extension decrease more than what could be expected from the predictions of a constant volume model because of the reduction of voids between the fibres. With the help of X-ray microtomography and an *in-situ* tensile machine designed for yarns, we experimentally measured the change of radius of the yarns during deformation as well as their average packing density over the cross-section. The predictions of the model, taking into account these experimentally validated contraction laws, are finally compared with macroscopic experimental tensile curves of these yarns.

The first section of this paper is devoted to the description of the single yarns studied and the experimental tests that were carried out to obtain their fibre orientations at rest and their packing density during extension. The theoretical background of yarn mechanics is then introduced including the use of fibre orientation distributions and deriving the non-linear yarn lateral contraction which takes into account the evolution of the fibre packing density. These two features (the orientation distribution and the packing density) are experimentally measured and fitted by means of appropriate functions in the third section. Finally, the yarn mechanical properties predicted are presented in the last section where the influence of the different parameters is discussed.

2. Materials and Method

2.1. Materials

Two types of fibres were used to produce continuous-filament yarns. The first bundle of a linear density of 144 tex (g/km), contains 384 polyester fibres. The second one contains 1000 aramid fibres and has a linear density of 167 tex (g/km). The bundles are twisted using a ring spinning machine to reach 3 different levels of twist : 100, 200 and 300 turns per metre (tpm). The aimed twist N_0, the diameter $d = 2r$ and the theoretical angle α at yarn surface ($\tan(\alpha) = 2\pi r N_0$) are gathered in Table 1. The actual twist measured after twisting the yarn is shown in brackets. Accurate mean values of the initial yarn diameters were measured with a Z-Mike laser.

Table 1: Single yarns produced and their geometrical parameters.

Type of fibre	Twist (tpm)	Diameter (mm)	α (°)
Polyester	100 (108)	0,48	9,2
	200 (195)	0,48	16,4
	300 (294)	0,48	23,9
Aramid	100 (105)	0,55	10,3
	200 (197)	0,55	18,8
	300 (297)	0,53	26,3

2.2. Experimental setup

A previous study from the same authors [10] about the fibre orientations in single and multi-ply yarns introduced the experimental setup that is used in the present article. X-ray microcomputed tomography is a non-destructive technique to obtain three-dimensional images of a sample at the microscopic scale [13]. Many radiographs are combined from different angular steps of the sample in front of the detector to build its 3D volume. An in-situ tensile machine was developed for the yarn prehension at rest and during its extension. The setup is controlled from outside the tomograph and all the data needed are stored in real time. These features allow yarns to be scanned in their initial configuration to obtain their orientation density functions (introduced in part 5) and at different steps during deformation in order to measure accurately the evolution of their radius. The voxel size is 2.6 μm for aramid fibres and 3.5 μm for polyester fibres with a scanning time of about 8 min. Even if the displacement speed is quite low (0.03 mm/min) for a gauge length of 4.5 cm, it is necessary to wait a short time before launching a scan because of the relaxation time of the sample, made of a polymer.

2.3. Measurement of the Yarn Packing Density

We assume a uniform packing density of the fibres over the yarn cross-section. This allows the packing density μ to be calculated as the ratio between the surface of the fibres S_f and the total area S_y of the yarn cross-section (containing the fibre cross-sections and the voids) :

$$\mu = \frac{S_f}{S_y} \tag{1}$$

The 4 steps leading to the value of the packing density are described in Fig. 1. First, a median filter is applied to the image obtained with X-ray microtomography and then, the images are binarized. A threshold must be chosen carefully in order to get the fibre cross-sections without cropping them or taking some voids into account. The value of the area of cross-sections S_f can show large variations (about 10%) depending on whether the threshold is under- or overestimated especially at large deformation when the fibres are very close to each other. Considering this point,

we choose to estimate the theoretical value of the surface S_f^{Th} of the fibre cross-sections rather than experimentally measuring it.

The equivalent radius R_b of a cylinder containing all the fibres of the original bundle without any void can be written as a function of the linear density Λ of the bundle and the specific weight ρ of the material :

$$R_b = \sqrt{\frac{\Lambda}{\pi\rho}} \tag{2}$$

The total surface of the section after twisting this compact cylinder is given by Leech [6] and its radius R_f^0 at rest is :

$$R_f^0 = R_b\sqrt{1 + (\pi N_0 R_b)^2} \tag{3}$$

where N_0 is the twist. Assuming that the fibres are incompressible, so their volume remains constant over their extension, allows the evolution of the radius R_f of the equivalent cylinder containing all fibres without void to be expressed as a function of the yarn deformation ϵ_y :

$$R_f(\epsilon_y) = R_f^0\sqrt{\frac{1}{1+\epsilon_y}} \tag{4}$$

Finally, knowing the theoretical total surface $S_f^{Th} = \pi R_f^2$ of the fibre sections and the experimentally measured total surface $S_y^{Exp} = \pi R_y^2$ of the yarn section as shown in Fig. 1d, the packing factor μ can be expressed as :

$$\mu(\epsilon_y) = \frac{S_f^{Th}}{S_y^{Exp}} \tag{5}$$

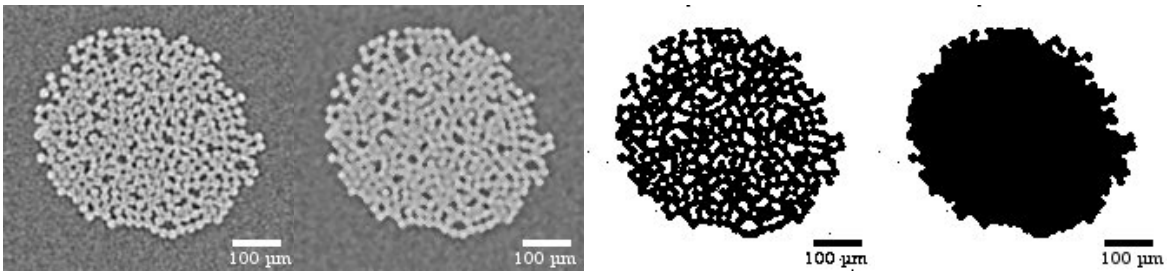

(a) (b) (c) (d)

Figure 1: (*a*) Image of a single yarn cross-section obtained with X-ray microtomography. (*b*) Median filter applied to the first image. (*c*) Binarization of the cross-section with an adapted threshold. (*d*) A function "fill holes" is applied to fulfil every blank hole between the binarized fibres.

3. Theoretical Background

In the following part, yarn mechanics will be developed on the basis of Leech's work [6] and linked with the theories involving a first key parameter : the orientation density functions which describe the yarn structure in a

statistical manner. From these derivations, another key parameter is underlined : the fibre deformation which depends on the fibre angle and on yarn lateral contraction. An expression is developed for the latter and unknown coefficients will be found by our experiments.

3.1. Yarn Mechanics

The energy functional per unit length U_f of a fibre should depend on its strain ϵ, its twist per unit length $\frac{d\theta}{ds}$ and its curvature χ. Following Liu [14] who showed that the contribution of fibre torsion and fibre bending in the total yarn stored strain energy are negligible compared to fibre tension and Leech [15] who neglected the energy dissipation due to friction, assuming that slippage between fibres remains very small in extension tests, we only take into account fibre tensile energy to derive the relationships. Hence, the energy functional U_f of a simple fibre can be written as :

$$U_f(\epsilon, \frac{d\theta}{ds}, \chi) = U_f(\epsilon) \tag{6}$$

If we deal with little portions of fibre being small enough to be considered as straight segments, we can sort each angle θ between fibre segments and the yarn axis (this angle will be called *fibre orientation*) into different intervals of an arbitrary width $\Delta\theta$ in order to obtain the relative frequency (probability) P of fibre orientations : $P(\theta, \Delta\theta) = \frac{n(\theta,\Delta\theta)}{N_s}$ where $n(\theta, \Delta\theta)$ is the number of angles falling into the range $\theta \pm \frac{\Delta\theta}{2}$ and N_s the total amount of fibre segments. The *Orientation Density Function* (ODF) $\omega(\theta)$ is defined by making the interval size $d\theta$ tend to zero as :

$$\omega(\theta) = \frac{P(\theta, d\theta)}{d\theta} \tag{7}$$

The structural strain energy per unit length for a yarn characterized by a distribution $n(\theta, \Delta\theta)$ of fibre orientations can be written as a function of U_f (energy/unit length) :

$$U_s = \sum_{0}^{\frac{\pi}{2}} n(\theta) \sec(\theta) U_f(\epsilon_f) \tag{8}$$

where $\sec(\theta)$ appears because of the obliquity of the fibres, increasing the volume of matter and thus, the stored fibre strain energy per unit length of yarn. In the continuous case, the previous relationship can be expressed in terms of the orientation density function $\omega(\theta)$:

$$U_s = N_f \int_0^{\frac{\pi}{2}} \omega(\theta) \sec(\theta) U_f(\epsilon_f) d\theta \tag{9}$$

This expression is the same as those developed first by Hearle and Sakai [7], and then by Komori and Makishima [5], who used a different definition of the orientation density function, but showed the equivalence with Hearle and Sakai.

Considering a yarn sample of initial length L_0 submitted to a tensile load F, the variation $L_0 dU_s$ of its strain energy induced by an infinitesimal increment of displacement dL can be calculated as:

$$L_0 dU_s = F \cdot dL. \tag{10}$$

The tensile force F can therefore be expressed as a function of the strain energy U_s as:

$$F = L_0 \frac{dU_s}{dL}. \tag{11}$$

As U_s is defined as a function of ϵ_f, the derivation of can be decomposed into:

$$\frac{dU_s}{dL} = \frac{dU_s}{d\epsilon_f}\frac{d\epsilon_f}{dL}. \tag{12}$$

Assuming a relation between the deformation of a fibre ϵ_f, and the axial strain of the yarn ϵ_s, one can write:

$$\frac{dU_s}{dL} = \frac{dU_s}{d\epsilon_f}\frac{d\epsilon_f}{d\epsilon_s}\frac{d\epsilon_s}{dL}. \tag{13}$$

Denoting L the current length of the yarn, and defining its axial strain by:

$$\epsilon_s = \frac{L - L_0}{L_0}, \tag{14}$$

one obtains:

$$\frac{d\epsilon_s}{dL} = \frac{1}{L_0}, \tag{15}$$

hence:

$$F = \frac{dU_s}{d\epsilon_f}\frac{d\epsilon_f}{d\epsilon_s}. \tag{16}$$

Then, introducing Eq. 9, the tensile force can be expressed as:

$$F = N_f \int_0^{\frac{\pi}{2}} \omega(\theta)\sec(\theta)\frac{dU_f}{d\epsilon_f}\frac{d\epsilon_f}{d\epsilon_s}d\theta. \tag{17}$$

We assume that the strain energy (energy/unit length) U_f of a fibre is equal to the strain energy of the bundle made of those fibres divided by their number N_f:

$$U_f(\epsilon_f) = \frac{1}{N_f}\int_0^{\epsilon_f} F_b(\epsilon)d\epsilon \tag{18}$$

Where F_b is the expression of the tensile force applied to the bundle as function of its elongation, which is experimentally identified. Whereas dispersion is expected in the experimental identification of the tensile response of individual fibres, approximating this response from a test performed on a bundle amounts to averaging the tensile behaviour over all fibres in the bundle, and is simpler than carrying out tests on single fibres. Finally, using the expression 18 in Eq.17, the total force F as a function of yarn deformation ϵ_y is :

$$F(\epsilon_y) = \int_0^{\frac{\pi}{2}} \omega(\theta)\sec(\theta)F_b(\epsilon_f)\frac{d\epsilon_f}{d\epsilon_y}d\theta \tag{19}$$

Sibellas et al. [10] investigated the experimental orientation density functions of various kinds of yarns (1 to 3 plies) and compared them to existing models. The same experimental setup was used with the same methodology to track the fibres in the single yarns studied here. The next section deals with the derivation of the expression of fibre deformation as a function of the yarn deformation taking into account yarn lateral contraction.

3.2. Fibre Deformation

The deformation of the fibre ϵ_f has to be expressed as a function of the yarn deformation ϵ_y. Considering sufficiently small portions of fibre so that they can be seen as straight segments, Hearle and Sakai [7] derived the deformation of these segments in space as a function of the initial fibre angle θ, the yarn deformation ϵ_y and the lateral contraction $\lambda(r)$ of the fibre segment:

$$\epsilon_f = \sqrt{(1+\epsilon_y)^2\cos^2(\theta) + (1-\lambda(r)\epsilon_y)^2\sin^2(\theta)} - 1 \tag{20}$$

The radial lateral contraction λ is defined as the ratio between the relative variation of radial position of the fibre and the axial deformation of the yarn :

$$\lambda(r) = -\frac{1}{\epsilon_y}\left(\frac{r}{r_0} - 1\right) \tag{21}$$

where r_0 and r are the radial position of the fibre in the initial configuration and after extension respectively. Assuming, for the sake of simplicity, a uniform contraction in the yarn cross-section, this lateral contraction can be expressed as a function of the yarn radius in the initial state R_0 and after deformation R :

$$\lambda = -\frac{1}{\epsilon_y}\left(\frac{R}{R_0} - 1\right) \tag{22}$$

The yarn packing factor μ is defined as the ratio between the surface of fibre sections and the total surface of the yarn section. This definition easily leads to the following relationship between the yarn radius and its packing factor at rest and under extension :

$$\frac{R}{R_0} = \sqrt{\frac{\mu_0}{\mu(\epsilon_y)}}\sqrt{\frac{1}{1+\epsilon_y}} \tag{23}$$

Hence, Eq. 20 can be rewritten as a function of the yarn packing factor :

$$\epsilon_f = \sqrt{(1+\epsilon_y)^2\cos^2(\theta) + \left(\frac{\mu_0}{\mu(\epsilon_y)(1+\epsilon_y)}\right)\sin^2(\theta)} - 1 \tag{24}$$

From this equation, we can derive ϵ_f in order to get the partial derivative in Eq. 19 :

$$\frac{\partial\epsilon_f}{\partial\epsilon_y} = \frac{1}{2(1+\epsilon_f)}\left[2(1+\epsilon_y)\cos^2(\theta) + \frac{\sin^2(\theta)}{\mu_0(1+\epsilon_y)^2}\left[\frac{d\mu(\epsilon_y)}{d\epsilon_y}(1+\epsilon_y) - \mu(\epsilon_y)\right]\right] \tag{25}$$

3.3. Yarn Rupture

The yarn mechanical model presented before will be used to evaluate the initial part of the tensile curves and does not aim at predicting their breaking point. Nevertheless, the rupture mechanism in the yarn is handled considering individually each class of orientations obtained in the experimental identification, and assuming a rupture criterion expressed in terms of the axial strain ϵ_{rupt} at the breaking point of the extension of the original bundle of parallel fibres (before being twisted). The axial strain ϵ_f of each individual class of orientation centred on a value θ is expressed as function of the axial strain of the yarn ϵ_y by means of Eq. 24. When this axial strain ϵ_f exceeds ϵ_{rupt} the tensile force for the corresponding class of orientations is set to zero.

3.4. Tensile Curve of the Initial Fibre Bundle

Experimental tensile curves of the initial fibre bundles (0 tpm) are difficult to obtain because of the lack of fibre cohesion. Moreover, single fibre tensile tests were not performed and their non-negligible variability would be a strong questionable aspect of the results. Instead, we performed tensile tests on the yarns twisted at 100 tpm and used the theory in an inverse manner to find an estimation of the bundle tensile curves. Taking the mean orientation angle $\bar{\theta}$ from the experimental orientation density functions at 100 tpm, we can rewrite Eq. 19 :

$$F_{100tpm}(\epsilon_y) = F_b(\epsilon_f)\sec(\bar{\theta})\frac{d\epsilon_f}{d\epsilon_y} \tag{26}$$

which gives :

$$F_b(\epsilon_f) = F_{100tpm}(\epsilon_y)\left[\sec(\bar{\theta})\frac{d\epsilon_f}{d\epsilon_y}\right]^{-1} \tag{27}$$

For each value of ϵ_y of the yarn at 100 tpm, we will find the value of F_b for the corresponding deformation $\epsilon_f = f(\epsilon_y)$. It should be noted that using the complete equation involving the orientation density function instead of the average angle $\bar{\theta}$ adds much more complexity in the determination of the tensile curve of the initial fibre bundle.

4. Experimental Measurements of the Evolution of the Packing Density

For each type of yarn (see table 1), measurement of their radius under extension was carried out with the help of the X-ray microtomography and the results are reported in Fig. 2a for the yarns made of polyester fibres and in Fig. 2b for the ones with aramid fibres. These figures show a non-negligible decrease of the yarn radius (about 10 % for the different cases) during the yarn extension.

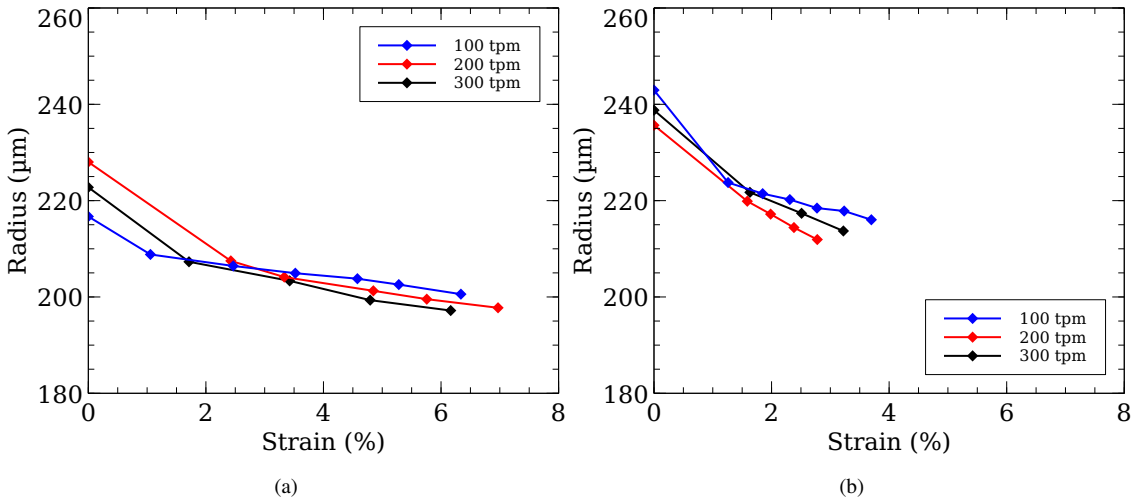

Figure 2: Evolution of yarn radius under extension in the case of (a) polyester fibres and (b) aramid fibres.

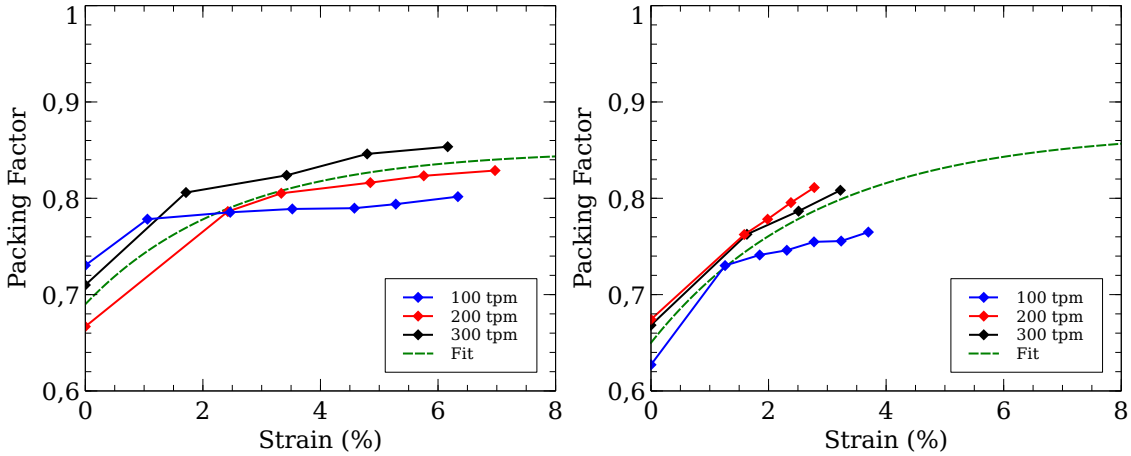

Figure 3: Evolution of the packing density under extension in the case of (a) polyester fibres and (b) aramid fibres.

The corresponding evolution of packing density for each kind of yarn is depicted in Fig. 3 where its increase with the yarn extension is clearly observed. The slope of the curve representing the evolution of the packing factor can be seen as a rate of contraction which is always the highest at the beginning of the deformation. This could be related to a high rearrangement of the fibres filling the empty spaces or straightening their curved parts instead of taking part in the yarn extension by elongating themselves. In addition, this rate of contraction is higher for aramid yarns which could be explained by the ratio between axial and flexural stiffness and the more important number of aramid filaments of a lesser size of radius. This combination tends towards a higher transverse pressure in the aramid yarn cross-section leading to a higher rate of contraction. The evolution of the packing density μ as a function of the yarn extension ϵ_y can be empirically fitted by the following expression :

$$\mu(\epsilon_y) = \mu_c + (\mu_0 - \mu_c)e^{-\kappa_\mu \epsilon_y} \tag{28}$$

where μ_0 is the initial value of packing density, μ_c the value of the packing density at infinite strain and κ_μ, a coefficient governing the rate of change of the packing density. The values of these parameters are adjusted so that the packing density function fits experimental data. For simplicity, it has been chosen to assume they are independent of the initial twist N_0, and to adjust them to fit the average of the experimental packing density curves obtained for three different twists (see Fig. 3). These adjusted values are summarized in table 2 and will be used in the following.

5. The Orientation Density Function

The orientation of a fibre represents the angle between its tangent (on a specific point of the fibre trajectory) and the yarn axis. Because of the stochastic character of the fibre arrangement and the consequent difficulty of deterministic models to describe the fibre trajectories in a realistic manner, orientation distributions are used to represent the

Table 2: Experimental parameters defining the evolution of the yarn packing density as a function of yarn extension.

Nature of fibres	μ_0	μ_c	κ
Polyester	0,69	0,85	40
Aramid	0,65	0,87	35

yarn structure. Accurate orientation distributions for single-ply and multi-ply yarns made of continuous fibres were obtained using X-ray microtomography by the same authors [10]. With the same experimental setup, yarns studied in this paper were scanned and their orientation distributions are depicted on Fig. 4b where the effect of twist increasing the obliquity of the fibres is clearly observed. These experiemental results will be used as input in the mechanical model described previously.

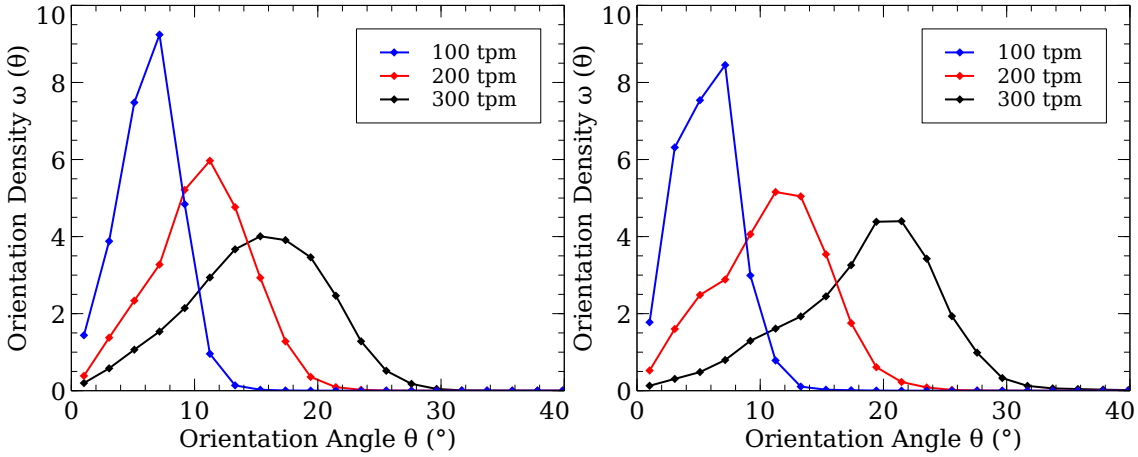

Figure 4: Orientation density functions of (a) polyester yarns and (b) aramid yarns.

6. Calculations of the Yarn Mechanical Properties

6.1. Tensile behaviour with a constant packing density

The forces developed by the yarns under extension were calculated with the orientation distributions described in the previous section and compared to experimental tensile curves. In order to firstly capture this influence independently of the lateral contraction (analysed in the next paragraph), the cross-sectional packing density of fibre μ is prescribed to be constant and equal to μ_0 in this first calculation. The results are reported in Fig. 5a for aramid yarns and in Fig. 5b for polyester yarns. We observe that each of the models can capture the decrease of stiffness with the twist but does not show an agreement with the experimental tensile tests. Thus, fibre orientations along with

a constant packing factor cannot explain the total decrease of rigidity of the yarn studied. Furthermore, the use of a distribution causes fibres with small orientation angles to break prematurely initiating cascading breaks of each of the class of fibre angle. The model described in this paper does not aim at modelling the last part of the tensile curve because it does not take into account the different phenomenons occuring before yarn rupture.

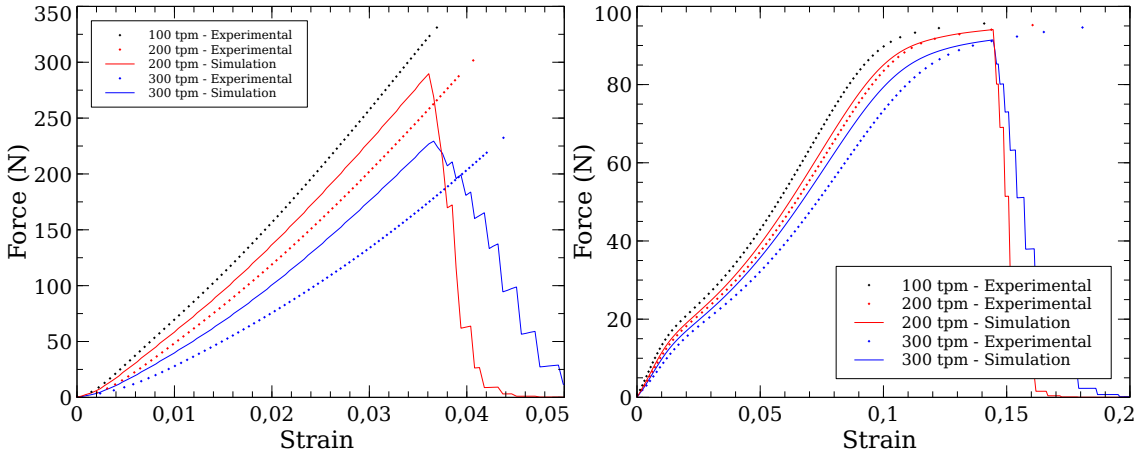

Figure 5: Influence of the orientation density function on (a) the whole tensile curve of aramid yarns and at (b) the beginning of the loading.

6.2. Tensile behaviour with a variable packing density

This last part is devoted to the calculation of the theoretical tensile curves with a variable fibre packing density determined experimentally (parameters are given in table 2). The results are reported on Fig. 6. In both case, very good agreements between the theoretical and experimental curves are obtained. Moreover, the strong non-linearity (arising from twist) of the yarn made of aramid fibres appears to be correctly predicted.

This variable fibre packing density allows fibres to take place in the empty spaces in the yarn cross-section during its extension, thus increasing the packing density. Consequently, the fibres can reduce their orientation angle towards the yarn axis and limit their own deformation. This induce a lower involvement of the fibres to the total longitudinal force developed and a lower overall rigidity of the yarn.

7. Conclusions

A model of the mechanical response during extension of single continuous-filament yarns based on the fibre orientation density function and a variable fibre packing density was presented. Those two key parameters were experimentally measured using X-ray microtomography, an in-situ tensile setup especially designed for yarns and different image processing techniques. Polyester and aramid fibres were twisted to produce yarns at 100, 200 and 300

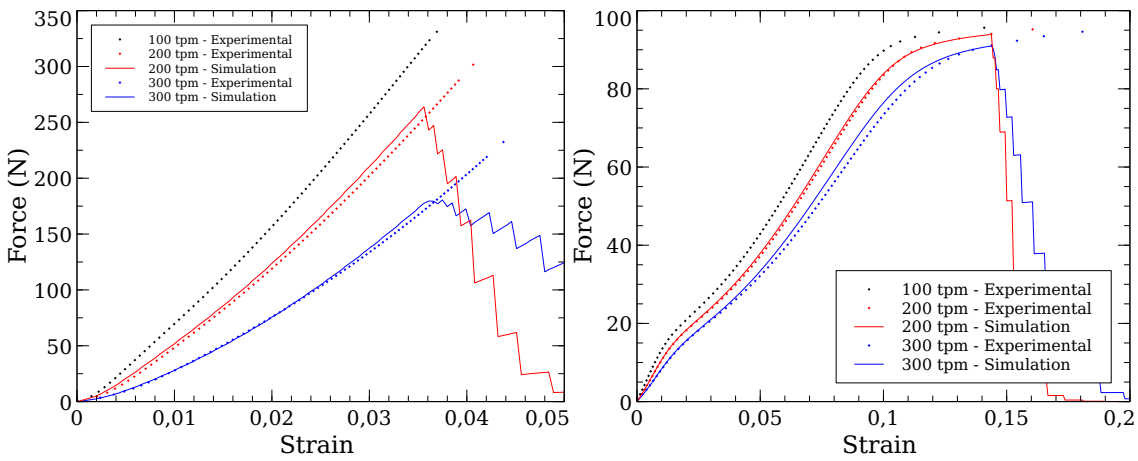

(a) (b)

Figure 6: Influence of the orientation density function on (a) the whole tensile curve of aramid yarns and at (b) the beginning of the loading.

turns per meter. The model showed that the fibre orientations and a constant packing density do not explain the total decrease of yarn rigidity. Taking into account the experimental variable fibre packing density through its theoretical derivation in the model led to very good agreements between theoretical and experimental curves and could predict the strong non-linearity of the tensile curves of yarn made of aramid fibres.

References

[1] J. Hearle, P. Grosberg, S. Backer, Structural Mechanics of Fibers, Yarns and Fabrics, Wiley-Interscience, New-York, 1969.

[2] L. Treloar, G. Riding, A theory of the stress-strain properties of continuous-filament yarns, Journal of the Textile Institute Transactions 54 (4) (1963) T156–T170. doi:10.1080/19447026308660166.

[3] N. Huang, G. Funk, Theory of Extension of Elastic Continuous Filament Yarns, Textile Research Journal 45 (1) (1975) 14–24. doi:10.1177/004051757504500103.

[4] J. Hearle, J. Thwaites, J. Amirbayat, Mechanics of dense fiber assemblies, in: Mechanics of Flexible Fibre Assemblies, Springer Netherlands, 1980, pp. 51–86.

[5] T. Komori, K. Makishima, M. Itoh, Mechanics of Large Deformation of Twisted-Filament Yarns, Textile Research Journal 50 (9) (1980) 548–555. doi:10.1177/004051758005000906.

[6] C. M. Leech, The modelling and analysis of the mechanics of ropes, Solid Mechanics and its Applications 209 (2014) 1–132. doi:10.1007/978-94-007-7841-2-1.

[7] J. Hearle, T. Sakai, On The Extended Theory of Mechanics of Twisted Yarns, Journal of the Textile Machinery Society of Japan 25 (3) (1979) 68–72.

[8] B. Jeon, J. Lee, A New Orientation Density Function of Ideally Migrating Fibers to Predict Yarn Mechanical Behavior, Textile Research Journal 70 (3) (2000) 210–216. doi:10.1177/004051750007000306.

[9] B. Jeon, Y. Kim, Orientation Density Function of Ply yarn, Textile Research Journal 80 (15) (2010) 1550–1556. doi:10.1177/0040517510363192.

[10] A. Sibellas, J. Adrien, D. Durville, E. Maire, Experimental study of the fiber orientations in single and multi-ply continuous filament yarns, Journal of the Textile Institute (2019). doi:10.1080/00405000.2019.1659471.

[11] W. Kilby, The mechanical properties of twisted continuous-filament yarns, Journal of the Textile Institute Transactions 55 (12) (1964) T589–T632. doi:10.1080/19447026408662251.

[12] N. Pan, Development of a Constitutive Theory for Short Fiber Yarns: Mechanics of Staple Yarn Without Slippage Effect, Textile Research Journal 62 (12) (1992) 749–765. doi:10.1177/004051759206201208.

[13] E. Maire, J.-Y. Buffière, L. Salvo, J. Blandin, W. Ludwig, J. Létang, On the application of X-ray microtomography in the field of materials science, Advanced Engineering Materials 3 (8) (2001) 539–546.

[14] T. Liu, K. Choi, Y. Li, Mechanical Modeling of Singles Yarn, Textile Research Journal 77 (3) (2007) 123–130. doi:10.1177/0040517507074022.

[15] C. Leech, The modelling of friction in polymer fibre ropes, International Journal of Mechanical Sciences 44 (3) (2002) 621–643. doi:10.1016/S0020-7403(01)00095-9.